

## WATER SORPTION IN A DEXTRAN GEL\*

JOHN A. TEXTER, RICHARD KELLERMAN†, AND KAMIL KLIER

*Department of Chemistry, Center for Surface and Coatings Research,  
Lehigh University, Bethlehem, Pennsylvania 18015 (U S A)*

(Received July 2nd, 1974, accepted in revised form, November 30th, 1974)

### ABSTRACT

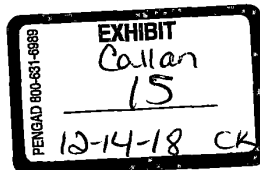
The state of adsorbed water in a dextran gel has been investigated by near-infrared and gravimetric-adsorption techniques. Water-vapor adsorption (desorption) isotherms at three temperatures are reported. The calculated sorption heats are found to be markedly temperature-dependent as well as dependent on the coverage. The near-infrared spectrum ( $4650\text{--}9000\text{ cm}^{-1}$ ) is reported, together with tentative assignments. The  $\text{H}_2\text{O}$  combination ( $\nu + \delta$ ) band at  $5184\text{ cm}^{-1}$  has been examined as a function of relative humidity. The line-shapes of this band have been analyzed by a recently established, Fourier-inversion technique, and information on the microdynamics of the adsorbed water molecules has been resolved on the picosecond time-scale. At low and intermediate degrees of hydration, reorientational jumps take place with periods from four to six times longer than those for free water. The onset of saturation is then accompanied by the sudden removal of the reorientational jumps. A comparison of microdynamical and thermodynamic data indicates the hydration mechanism to be highly cooperative at all relative humidities.

### INTRODUCTION

The study of water-carbohydrate interactions remains an important area of research, as such interactions are ubiquitous in biological systems and significant in many industrial applications. Cellulose-water interactions have been intensively studied for over three decades and have been extensively reviewed<sup>1-3</sup>. Starch-water interactions have been studied by n.m.r.<sup>4-7</sup>, isothermal water-vapor adsorption (desorption)<sup>8-13</sup>, and deuterium exchange<sup>14</sup> techniques. Northcote pointed out<sup>15</sup> the physiological importance of water-carbohydrate interactions in his early comparisons of water-vapor sorption by dextran, a variety of glycogens, and assorted yeast cell-wall carbohydrates. Agar gel-water interactions have been investigated by n.m.r. methods<sup>16</sup>, and amylose hydration has been studied by X-ray and deuterium-exchange techniques<sup>14,17</sup>. Hydration of dextran has been reinvestigated by X-ray and isothermal vapor-sorption methods<sup>13,18</sup>. Many carbohydrate polymers are non-rigid and exhibit significant swelling with increasing water content. In addition, their water-

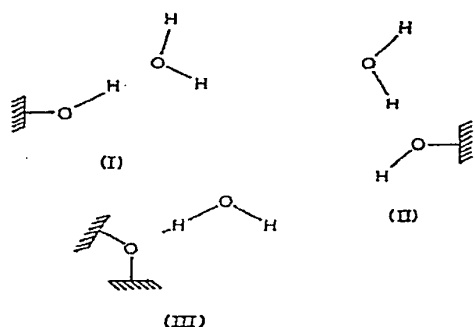
\*Supported, in part, by a Gulf Summer Research Fellowship to J. A. Texter.

†Present address: Xerox Corporation, 800 Phillips Road, Building 114, Webster, New York 14580



vapor adsorption-desorption isotherms often undergo marked hysteresis, which effects have usually been interpreted in terms of capillary-condensation theories<sup>11 12 15</sup> and steric rearrangements<sup>2 9 10 17</sup>

These hysteresis effects raise significant questions regarding the *mechanism* of carbohydrate hydration (dehydration) and associated swelling phenomena. Some of these questions are: To which functional groups of the saccharide monomer and cross linkages do adsorbed water molecules bind? What is the sequence of hydration of the different functional groups? What are the strengths (heats) of these interactions? Are the bound water molecules attached as hydrogen-bond acceptors (I) or as hydrogen-bond donors (II and III)?



Additional questions pertain to the microdynamics of adsorbed water. What is the rotational freedom (restriction) of the adsorbed water molecules? How are the microdynamics of the adsorbed water molecules *modulated* by the perturbing potential field of the adsorption sites and surrounding functional groups (and neighboring water molecules)?

We report herein the results of near-infrared and water-vapor adsorption (desorption) studies on the state of adsorbed water in a model carbohydrate system, a dextran gel (Sephadex® type G-15 gel, Pharmacia Fine Chemicals, Inc.) This swelling molecular sieve has found wide usage over the past fifteen years in many biochemical purification and chromatographic procedures.<sup>19</sup> In addition to structural or conformational effects, the question of solvent ( $H_2O$ ) effects in this gel on its relative selectivity to adsorb a number of aldoses and other substances has been raised previously by Marsden<sup>20</sup>. The type G-15 gel (hereafter referred to simply as "gel") utilized in this investigation is formed into spherical beads (40–120  $\mu m$  in diameter when dry) by tightly crosslinking dextran strands (produced by various strains of *Leuconostoc mesenteroides*) with 2,3-epoxypropyl chloride. This results in 2-hydroxypropan-1,3-diyl cross-linkages between dextran strands.<sup>20</sup> At 100% relative humidity the gel swells to a bed-volume of 2.5–3.5 ml per g of dry gel. The structure of dextran is largely characterized by its primary (1→6)- $\alpha$ -D-glucan backbone. The linkage points and lengths of the secondary side-chains of D-glucose residues have

been investigated by several research groups<sup>21-25</sup>. The i r analysis of carbohydrates has been reviewed by Neely<sup>26</sup>. The i r and Raman spectra of various carbohydrates, including  $\alpha$ -D-glucose and dextran, have been reported by several workers<sup>27-31</sup>. Analysis of  $\alpha$ -D-glucose in the fundamental i r region has indicated that most of the monomer modes are highly coupled<sup>28</sup>. Other i r evidence<sup>31</sup> indicates little if any intramolecular hydrogen-bonding (at least in crystalline monosaccharides).

The near-i r portion of this study consists in the main of monitoring the  $\nu + \delta$  combination-band ( $5100\text{--}5300\text{ cm}^{-1}$ ) of water adsorbed on the gel as a function of relative humidity ( $P/P_0$ ). This combination band arises from the  $\nu_2(\delta)$  and  $\nu_3$  fundamental vibrational modes of molecular water. Analysis of this  $\text{H}_2\text{O}(\nu + \delta)$  band



has been successfully utilized in characterizing many features of water interactions with silicas, silicates, and aluminosilicates<sup>32, 33</sup>. In particular, band-center shifts and band asymmetry (induced by inhomogeneous broadening) may be used to characterize the type of hydrogen bonding (donor or acceptor) and the average potential-field perturbing the rotational relaxation of the adsorbed water molecules.

It was shown by Gordon<sup>34</sup> that the normalized, inverse Fourier transform (real part) of vibrational i r spectra yields an autocorrelation function  $C(t)$  for the transition-moment dipole

$$C(t) = \frac{\int_{\text{band}} \cos \omega t I(\omega) d\omega}{\int_{\text{band}} I(\omega) d\omega}$$

This autocorrelation function may be interpreted as an ensemble average (over the three polarization directions) of the projection of a unit vector in the direction of the transition-moment dipole at time  $t$  onto itself at time zero. The vibrational-band intensity  $I(\omega)$  is expressed as a function of angular frequency-displacement from the band maximum. Such analysis yields significant microdynamical information on the rotational relaxation of the functional group(s) giving rise to the absorption, if the geometrical relation of the transition-moment dipole to the skeletal structure is known. This technique has of late been applied to a variety of organic substances in characterizing their rotational-diffusion mechanisms, which studies have recently been reviewed<sup>35</sup>. Wall<sup>36</sup> has applied the technique to a characterization of O-H and O-D stretching modes in bulk water based on Raman spectra. The general theory has recently been extended<sup>33</sup> by a first-order perturbation treatment to account for inhomogeneous broadening, as evidenced by asymmetry in the rotational structure of the vibrational-rotational absorption bands. The potential field  $\hat{V}(\mathbf{r}, t)$  perturbing the vibrational-rotational motion of the adsorbed water molecules interacts differently with the ground and excited vibrational-rotational states, hence the inhomogeneous broadening occurs. The observed line-shape for adsorbed water is thus found to

contain valuable information on the rotational relaxation and therefore provides an indirect estimate of the average potential-field perturbing the molecular motion. The  $\nu + \delta$  band is ideal for this kind of analysis, as the transition-moment dipole lies nearly in the molecular-water plane perpendicular to the molecular dipole (compare the  $\nu_2$  and  $\nu_3$  normal modes). In addition, the dynamical motion may be resolved (0–10 psec) to a degree hardly approached by nmr dynamical estimates. The correlation-function approach is thus seen to provide a powerful probe for mechanistic studies of water interactions with carbohydrates (as well as with other substances).

Water-vapor adsorption (desorption) isotherms give a direct estimate of the hydrophilicity of the gel as a function of relative humidity. When isotherms are recorded at different temperatures, heats of adsorption (desorption) may be estimated as a function of (water) coverage by use of the Clapeyron–Clausius relation. The results reported here of the vapor-sorption isotherms and near-ir  $\text{H}_2\text{O}$  ( $\nu + \delta$ ) spectra of water adsorbed on the gel are correlated with one another, and a mechanism for the hydration of the gel is proposed.

#### EXPERIMENTAL

*Preparation of samples* — The type G-15 gel was used as received. The samples for adsorption and spectral measurements were first dehydrated by heating for 48 h at 378°K *in vacuo*.<sup>20</sup> This treatment was confirmed to be sufficient by the absence of any detectable absorption in the 5100–5300  $\text{cm}^{-1}$  region due to water and by the attainment of constant weight on the adsorption (spring balance) apparatus. The small peak at 5240  $\text{cm}^{-1}$  (compare Fig. 1) may be due to a small amount ( $< 5 \times 10^{-4}$  g of water per g of gel) of tightly bound water that is unaffected by the dehydration procedure described. The gel began to decompose at 393°K.

*Sorption isotherms* — Water-vapor adsorption (desorption) isotherms were obtained by using the McBain–Bakr spring-balance technique.<sup>37</sup> A quartz spring having a spring-constant of 0.9779 mg/mm was used. A 62.65-mg sample of the gel (dry weight) was suspended from the spring in a quartz bucket by a quartz filament. The distension of the spring was measured with a Gaertner (Chicago, Illinois) travelling telescope whose vertical displacement could be read to better than  $\pm 0.0025$  mm. The water-vapor reservoir was filled with distilled water and deoxygenated by repeated freezing (at 77°K) and thawing under vacuum. The water-vapor pressure was monitored with an oil (Apiezon B) manometer. The density of the oil was determined to be 0.875 g/ml by using a Weld pycnometer. The reference arm of the manometer was kept at less than  $10^{-3}$  torr via a zeolite 13X sorption pump. Adsorption (desorption) isotherms were recorded at 284, 299, and 329°K. The water-vapor reservoir was maintained at the ambient temperature (299°K) during all measurements. The measurements at 284°K were made with the bottom of the spring-tube submerged in a bath of refrigerated methanol. A cylindrical furnace was used to maintain constant temperature for the measurements at 329°K. The data from the measurements at 284 and 329°K were corrected for thermal-flow effects by using a 62.75-mg Pyrex cane weight suspended in the bucket instead of sample.

*Spectroscopy* — The near-i r spectra were recorded with a Cary 14R recording spectrophotometer in dispersed-diffuse illumination mode by using a double-beam reflectance attachment and a 0-2.4 absorbance unit slide-wire. The sample was placed in a quartz reflectance cell similar to that described elsewhere<sup>38</sup>, except that the cell was not surrounded by a thermostating jacket. The sample spectra were recorded against a dehydrated standard of magnesium oxide placed in an identical cell after the baseline had been set. The baseline was set by balancing the spectrophotometer output with identical dehydrated magnesium oxide cells placed in the sample and reference beams. The sample cell was maintained under vacuum and equilibrated with water at sequentially higher vapor pressures in an adsorption apparatus described earlier<sup>32</sup>.

The sample equilibration and spectral measurements were performed at 297°K. The recorder output of the spectrophotometer was equipped with a digital interface to facilitate the numerical treatment of the spectra. The reflectance  $R_\infty$  (ratio of total intensities of radiation reflected from the sample and that reflected from the magnesium oxide standard) was obtained directly from the recorder output ( $-\log R_\infty$ ) and transformed by using Schuster-Kubelka-Munk theory<sup>38-40</sup> to obtain the ratio of the absorption to scattering coefficients  $F(R_\infty)$  according to the transformation.

$$F(R_\infty) = \frac{(1 - R_\infty)^2}{2 R_\infty} = \frac{K}{S}$$

The scattering coefficient ( $S$ ) was judged to be independent of frequency over the intervals measured on the basis of the isotropic nature of the spherical sample-beads and the coincidence of the adsorbed-water ( $\nu + \delta$ ) spectrum at high relative humidity with that of bulk water. The  $F(R_\infty)$  spectra are thus equivalent to absorption spectra, but for a multiplicative constant  $1/S$ . Spectra equivalent to absorption spectra, but for an additive constant  $-\log S$ , are obtained from  $\log F(R_\infty)$ . The gel is a swelling polymer and, therefore, excluded-volume effects must be considered. The absorption coefficient  $K$  may be considered as the product ( $c\kappa$ ) of concentration ( $c$ ) and molar absorption-coefficient ( $\kappa$ ) terms. Excluded-volume effects are therefore obviated, as the representation  $\log F(R_\infty)$  yields spectra identical to absorption spectra, but for an additive constant  $\log(c/S)$ .

Spectra in the fundamental region were recorded on a Perkin-Elmer 257 grating instrument for the purpose of comparison with dextran and other D-glucose-related spectra. A pellet technique was used with 6 mg of gel and 60 mg of spectral-grade potassium bromide being compressed into a pellet 1 cm in diameter. The spectrum was recorded in transmission mode with a comb attenuating the reference beam.

*Numerical* — All numerical treatments of the spectra were carried out in FORTRAN code with a CDC 6400 electronic computer. The near-i r spectra were sampled at 1-nm intervals, recorded on punched-paper tape, and then transferred to magnetic tape for processing by the computer. The inverse Fourier-transforms of the  $\nu + \delta$  bands were computed by making straightline interpolations between recorded



ordinate-abscissa pairs, and performing the integration (at each time-value) in closed form in a stepwise manner. The wavenumber abscissa-values were scaled to have units of angular frequency (displaced from the band maximum)

#### RESULTS AND DISCUSSION

*Near-i r spectrum.* — The near-i r spectrum of the dehydrated gel is illustrated in Fig. 1 over the  $4650\text{--}9000\text{ cm}^{-1}$  interval. Many bands and shoulders are discernible, and assignments are attempted for some of these on the basis of the pellet spectrum in the fundamental region (Table I), whose assignments are based on various studies on monosaccharides and dextran, as noted in the Introduction. The most intense near-i r. band occurs at  $4770\text{ cm}^{-1}$ . This is probably due to a combination of the O-H stretch at  $3400\text{ cm}^{-1}$  with admixtures of C-H deformation,  $\text{CH}_2$  scissor, and C-O stretch modes. There is no band at  $5100\text{ cm}^{-1}$  as has been reported for dextran<sup>30</sup>, this assignment was probably made due to the presence of adsorbed water. The broadened peaks in the  $5500\text{--}5900\text{ cm}^{-1}$  interval may arise from combination of the O-H stretching fundamental with admixtures of the first overtones of the C-O stretch and O-H deformation modes ( $2100\text{ cm}^{-1}$ ). The  $6400\text{ cm}^{-1}$  band arises out of combination of the O-H stretch with the methylene stretching mode at  $2880\text{ cm}^{-1}$ . The more-intense peak at  $6900\text{ cm}^{-1}$  is undoubtedly the first overtone of the O-H stretching mode whereas the broad, weak band at  $8270\text{ cm}^{-1}$  might be attributable to admixture of the  $6900\text{ cm}^{-1}$  overtone with the  $\text{CH}_2$  scissor fundamental. Some of these assignments should hardly be considered more than speculative. However, the high density

TABLE I

INFRARED SPECTRUM OF DEXTRAN GEL<sup>a</sup>

Band position ( $\text{cm}^{-1}$ )	Intensity	$\Delta\tilde{\nu}_{1/2}$ ( $\text{cm}^{-1}$ ) <sup>b</sup>	Assignment
3400	v	400	O-H stretching (including some adsorbed water) <sup>c</sup>
2880	s	130	methylene C-H stretching
2100	w	100	admixture of C-O stretching and in-plane O-H deformation overtones
1635	w	120	adsorbed water
1455	m		$\text{CH}_2$ scissor
1400	w		
1350	m		C-H deformation
1330	m		
1265	m		C-O stretching
1100	s		O-H deformation
930	w		C-H stretching
870	w		this region is extensively broadened due to "lattice"
770	w		mode coupling

<sup>a</sup>Pellet sample prepared as described in the experimental section. <sup>b</sup>Bandwidth at half-maximum intensity. <sup>c</sup>The pellet sample was not subjected to the dehydration procedure.

of states illustrated in the near-ir unequivocally reiterates the previous contention<sup>28</sup> that vibrational modes of dextran are highly coupled. The 5000–5400  $\text{cm}^{-1}$  interval of the near-ir spectrum of the dehydrated sample is relatively flat, and therefore quite suitable for analysis of the  $\text{H}_2\text{O}$  ( $\nu + \delta$ ) band

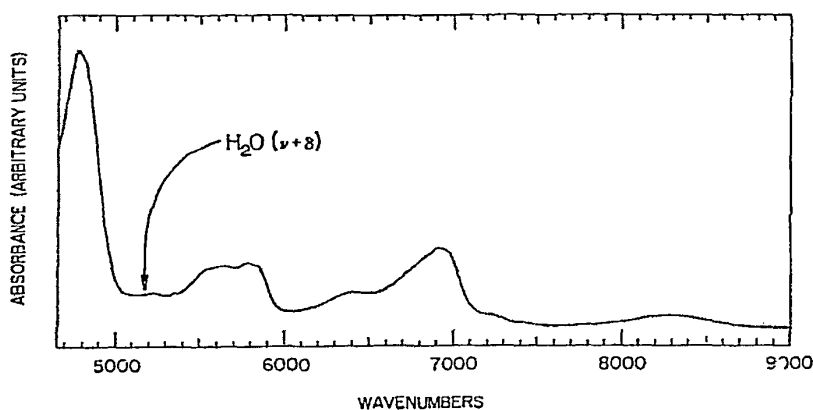


Fig 1 Near infrared spectrum of dehydrated dextran gel. The arrow indicates the position of the  $\text{H}_2\text{O}$  ( $\nu + \delta$ ) combination-band when water is adsorbed on the gel. Spectrum recorded at 297°K. The ordinate is depicted in arbitrary  $F(R_\infty)$  absorbance units.

Fig 2 illustrates representative  $\text{H}_2\text{O}$  ( $\nu + \delta$ ) spectra recorded at different relative humidities. The spectrum of the dehydrated sample was subtracted from each of the recorded  $\nu + \delta$  bands, after which a baseline connecting the band wings was subtracted. The peak-maximum position, half-width at band maximum, intensity at band maximum, integrated band-intensity, and correlation times as estimated from  $\Delta\tilde{\nu}_{1/2}$  are illustrated in Table II (columns 1, 3, 4, 5, 6, and 8) for all of the spectra recorded. The position of the peak maximum stays relatively constant at 5184  $\text{cm}^{-1}$ , with minor excursions to lower frequencies at 1% and 27–55% relative humidity. The change in band asymmetry with changing  $P/P_0$  for the spectra illustrated in Fig 2 is noteworthy.

**Correlation functions** — The correlation functions computed from the near-ir spectra ( $\nu + \delta$  band) of the gel sample, equilibrated at various humidities, are illustrated in Figs 3-a, -b, and -c over the 0–0.5 picosecond time-interval. There is some ambiguity in the experimental choice of frequency zero for the rotational correlation-functions with angular coupling, as the position of the vibrational band-center is not exactly known and does not necessarily coincide with the vibrational band-maximum. However, such an ambiguity is removed by following the total correlation-function (including vibrations) obtained by Fourier inversion with frequency measured from the *actual* frequency zero rather than by using frequency centered at the vibrational band-center. The perturbed, rotational correlation-function is then an *envelope* of the total correlation-function<sup>33</sup>. The correlation

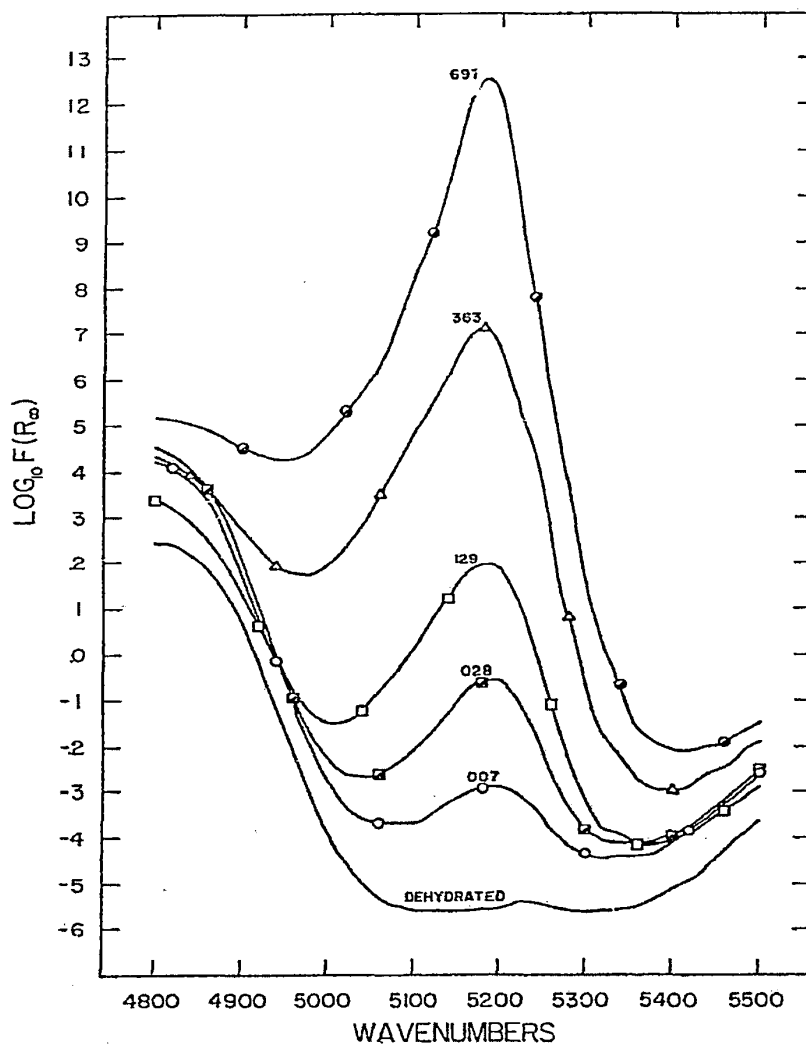


Fig. 2. The  $\text{H}_2\text{O}$  ( $\nu+\delta$ ) band of water adsorbed on gel at representative relative humidities ( $P/P_0$ ) of 0.007, 0.028, 0.129, 0.363, and 0.697. Note the change in band shape with changing water-content. Spectra recorded at  $297^\circ\text{K}$ .  $P_0 = 22.4$  torr. The circles, triangles, and squares are not data points but are intended to aid identification of the spectra in the wings of the bands. The spectra were sampled at  $1\text{-nm}$  intervals.

functions centered at vibrational band-maxima corresponded *excellently* with the envelopes of the total correlation-functions, and therefore no further search was made for the exact vibrational band-centers. We therefore consider these functions to be reliable over the illustrated time-interval of  $0.5\text{ psec}$ , as the experimental spectral resolution of about  $3\text{ cm}^{-1}$  should yield functions reliable up to  $10\text{ psec}$ <sup>33</sup>. The experimental error of the correlation functions was computed by carrying the standard



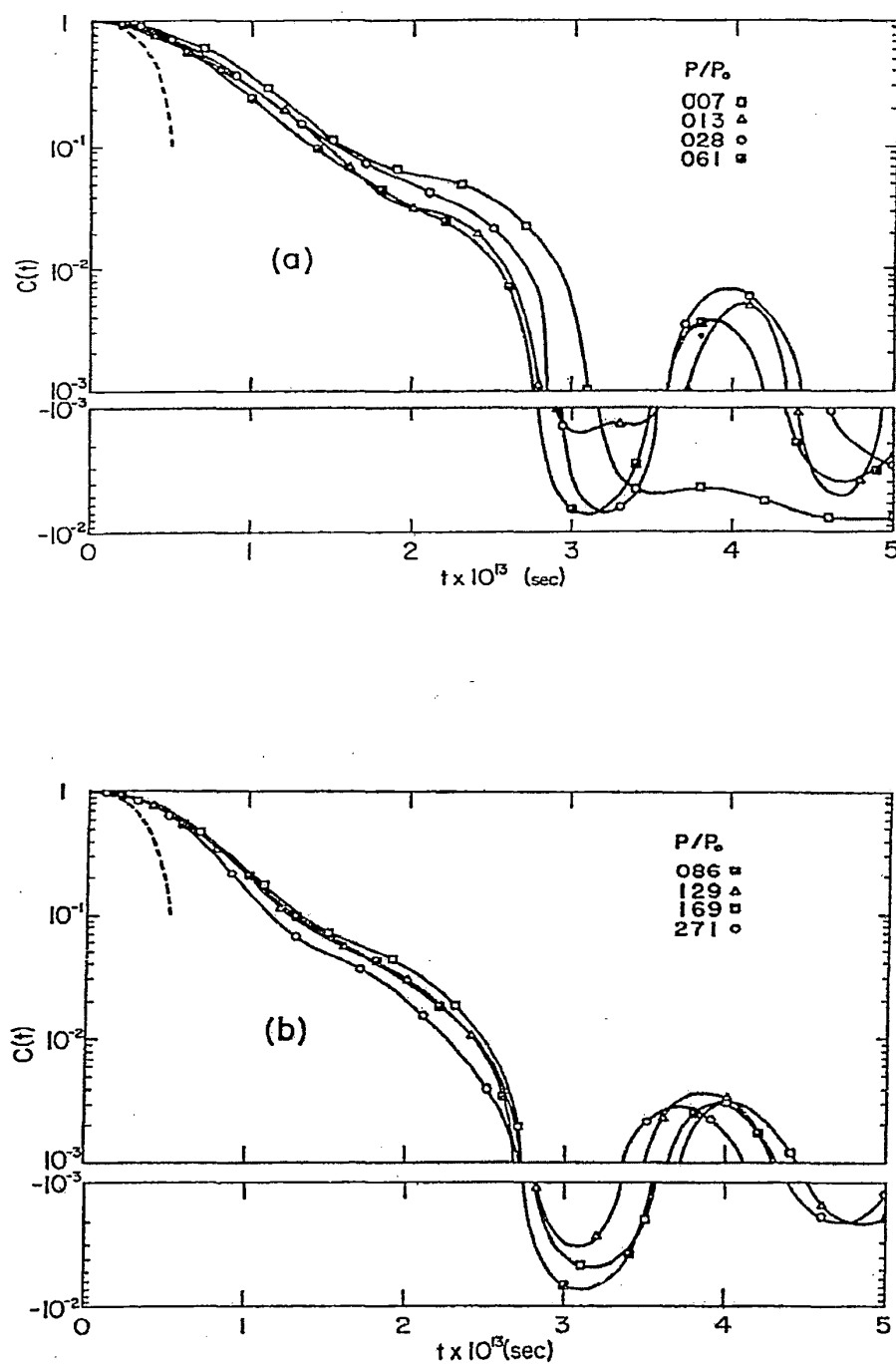


Fig 3.

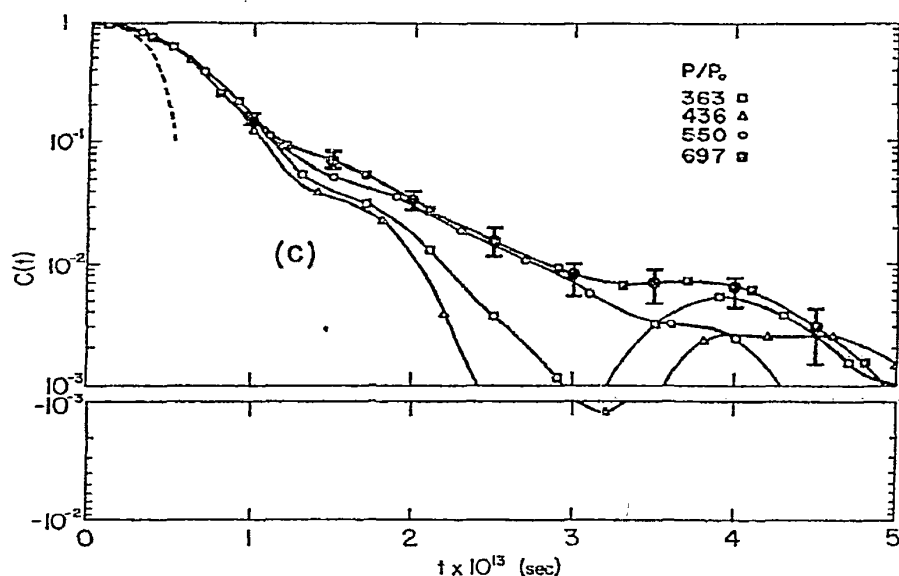


Fig 3 Rotational correlation-functions for  $(\nu + \delta)$  transition-moment dipole of water adsorbed on dextran gel at different relative humidities ( $P/P_0$ ) (a)  $P/P_0 = 0.007, 0.013, 0.028$ , and  $0.061$ , (b)  $P/P_0 = 0.086, 0.129, 0.169$ , and  $0.271$ , and (c)  $P/P_0 = 0.363, 0.436, 0.550$ , and  $0.697$ . The dashed line is the classical correlation-function  $C(t) = 1 - kTt^2/I_A$  valid at short times, where  $I_A$  is the least inertial moment of molecular water ( $I_A = 1.024 \times 10^{-40} \text{ g cm}^2$ ).  $P_0 = 22.4 \text{ torr}$ . The error bars illustrated for the  $P/P_0 = 0.697$  correlation function are representative of the computed error for the other correlation functions. Note that the computed error approaches zero (although nonuniformly) in the limit of large time, as expected for the average product-area of  $\int \cos(\omega) f(\omega) d\omega$  ( $f$  arbitrary and continuous) and in conformance with the limit  $C(t) \rightarrow 0$  for  $t \rightarrow \infty$ .

deviation (as a function of frequency) of the recorder output ( $-\log R_\omega$ ) for the multiply scanned spectra (3 to 5 scans were made at each relative humidity) through the transformation  $F(R_\omega)$  and the Fourier inversion for  $C(t)$ . The absolute error indicated by the bars in Fig 3-c for the case  $P/P_0 = 0.697$  is representative of the reliability of the correlation functions illustrated.

The differences in the correlation functions at different relative humidities is striking, and the rotational relaxation is certainly anything but exponential. It is noteworthy that all of the correlation functions decay more *slowly* than the fastest possible motion of a classical free rotor (dashed line). This is significant as compared to *bulk* water, whose correlation function (below the critical temperature) decays more *rapidly* than the classical motion<sup>33</sup>. Another general feature characterizing all of the illustrated correlation-functions is the inflection that occurs in the 0.1–0.2 psec interval. This indicates that the adsorbed water molecules move in a field that alternately accelerates and decelerates the rotational diffusion.

The behavior of the correlation function at 0.7% relative humidity is interesting, as it illustrates the existence of a significant rotational barrier. Note that this function

TABLE II

EQUILIBRIUM AMOUNTS OF ADSORBED WATER AND FREQUENCIES,  
BAND WIDTHS AT HALF-MAXIMUM, INTENSITIES, AND CORRELATION TIMES ( $\tau_c$ ) FROM  
RECORDED  $H_2O$  ( $\nu + \delta$ ) BANDS

$P/P_0^a$	$g H_2O/g\ gel^b$	$H_2O$ ( $\nu + \delta$ ) Band				Correlation times $\times 10^{13}$ (sec)	
		$\tilde{\nu}_{max}(cm^{-1})$	$\Delta\tilde{\nu}_{1/2}(cm^{-1})$	$I_{p_{max}}^c$	$\Sigma I^f$	$\tau_c(\Sigma)^e$	$\tau_c(\Delta\tilde{\nu}_{1/2})^d$
0.007	0.003	5184	167	0.166	0.568	3.71	2.00
0.013	0.005	5180	190	0.278	1.086	3.22	1.75
0.028	0.009	5184	180	0.393	1.460	3.41	1.85
0.061	0.027	5184	201	0.510	2.092	3.10	1.66
0.086	0.039	5184	218	0.567	2.441	2.95	1.53
0.129	0.055	5184	221	0.685	2.962	2.94	1.51
0.169	0.066	5184	210	0.841	3.464	3.07	1.59
0.271	0.090	5181	239	0.872	4.042	2.72	1.40
0.363	0.114	5179	267	1.097	5.140	2.68	1.25
0.436	0.132	5181	256	1.098	5.401	2.56	1.30
0.550	0.168	5176	238	1.346	6.116	2.77	1.40
0.697	0.248	5184	239	1.574	7.325	2.71	1.40

<sup>a</sup>From near-i.r. spectra equilibration-runs at 297°K,  $P_0 = 22.4$  torr <sup>b</sup>Adsorbed amounts from isotherm recorded at 299°K,  $P_0 = 25.2$  torr <sup>c</sup>Correlation time estimated from rotational correlation-function by summing the positive area under the correlation function over the interval of 0–0.5 picoseconds <sup>d</sup>Correlation time estimated from inverse of bandwidth at half-maximum intensity <sup>e</sup>Intensities, expressed in  $\log F(R_\infty)$  units, with spectrum of the dehydrated sample and baseline connecting wings of the band subtracted from the experimental spectrum <sup>f</sup>Integrated intensities over the recorded ( $\nu + \delta$ ) band-interval (arbitrary units)

initially decays more slowly than all of the rest and once having diffused more than  $\pi/2$  radians does not (in the time-interval illustrated) rotate back

All of the correlation functions illustrated indicate diffusion by  $\pi/2$  radians, but the time required to achieve this amount of rotation is not monotonic with increasing  $P/P_0$ . The general trend for the time ( $t_{\pi/2}$ ) required to first diffuse by  $\pi/2$  radians is that it decreases as  $P/P_0$  rises from 0.007 to 0.436, at which point  $t_{\pi/2}$  suddenly increases with increasing  $P/P_0$  (see Table III)

The correlation functions at initial times are illustrated in Fig. 4. Their behavior is to be contrasted with the classical correlation-functions describing free rotations about the three principal moments of inertia of molecular water,  $I_A$ ,  $I_B$ , and  $I_C$ .<sup>4,1</sup> The times required for rotational diffusion through  $9\pi/200$  radians ( $8.1^\circ$ ) are listed in Table III. Again, the behavior of  $t_{9\pi/200}$  is not monotonic with increasing  $P/P_0$ , but the general trend indicates the initial decay to be faster with increasing coverage, which is consistent with the fact that bulk water decays initially faster than the fastest possible classical decay (compare  $I_A$  in Fig. 4).

The integrated correlation-times ( $\tau_c$ ) are illustrated in Fig. 5 and listed in Table II (column 7) as a function of  $P/P_0$ . It may be noted that  $\tau_c$  shows the same general decrease as  $t_{\pi/2}$  to a minimum at  $P/P_0 \approx 0.45$ , followed by an abrupt increase. These times are to be compared with those estimated from the bandwidths at half-

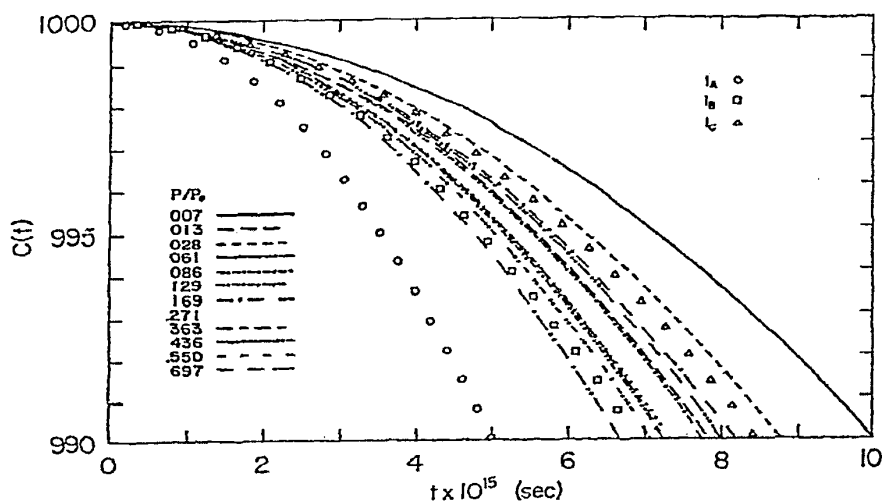


Fig 4 Short-time behavior of rotational correlation-functions at various water coverages. Note that the motions at 8.6 and 12.9% relative humidity are identical on this scale. The rotations are compared with the classical decay about the three principal inertial moments of the water molecule  $I_A$ ,  $I_B$ , and  $I_C$  are  $1.024$ ,  $1.920$ , and  $2.947 \times 10^{-40} \text{ g cm}^2$  respectively.  $P_0 = 22.4 \text{ torr}$

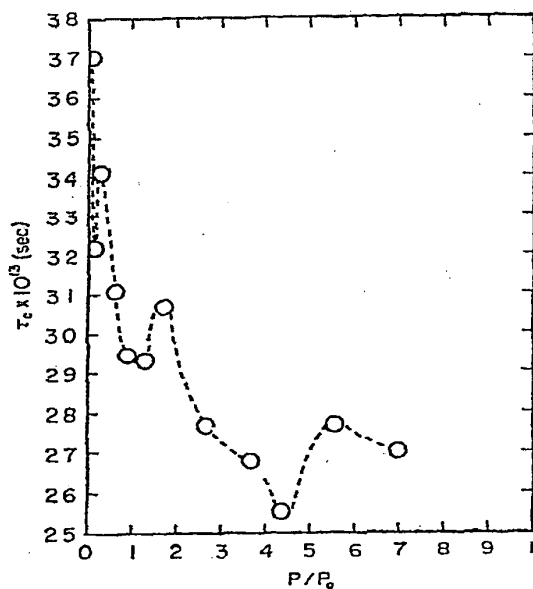


Fig 5 Rotational correlation-times of water adsorbed on dextran gel as a function of relative humidity ( $P/P_0$ ), computed according to note <sup>c</sup> in Table II.  $P_0 = 22.4 \text{ torr}$

maximum intensity. Interestingly, the latter are shorter than those measured by direct integration of the correlation function by  $48 \pm 5\%$ , over the measured  $P/P_0$  interval. Both of the  $\tau_c$  values ( $\Sigma$  and  $\Delta\tilde{\nu}_{1/2}$ , compare Table II) show the same "bumping" illustrated in Fig 5. This shows that the relative changes of both correlation times have physical meaning as a measure of rotational relaxation.

**Isotherms and sorption heats** — The adsorption-desorption isotherms recorded at three different temperatures are illustrated in Fig 6 ( $P_0 = 25.2$  torr). The hysteresis characteristic of swelling carbohydrates is noteworthy. Extrapolation of the desorption isotherms indicates that 5 mg of water per g of gel is irreversibly bound to the gel. Most of this water is removed, however, by the dehydration treatment described in the experimental section. At 299°K the gel begins to become saturated above 40% relative humidity.

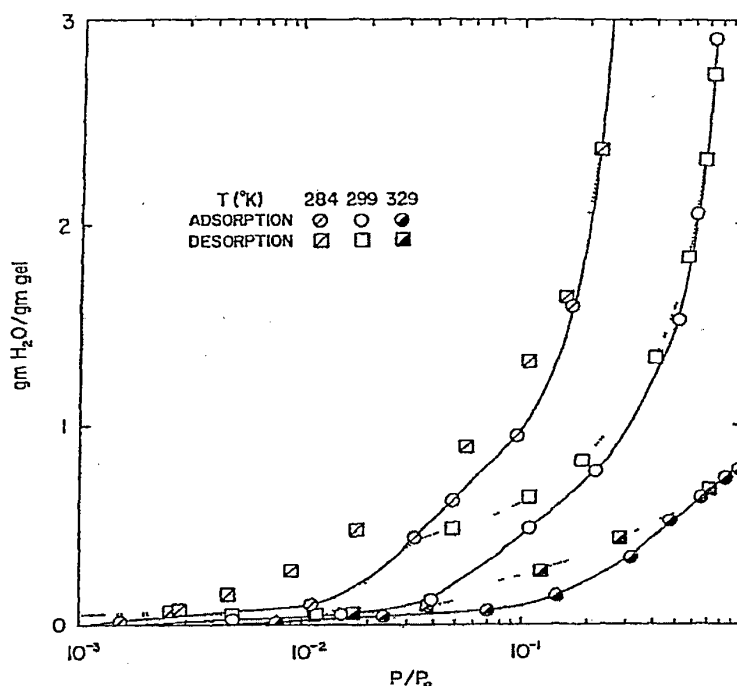


Fig 6 Adsorption-desorption isotherms for water on dextran gel at 284, 299, and 329°K.  $P_0 = 25.2$  torr

Isotherms are often recorded spectroscopically by plotting the peak-maximum intensity or sum of peak intensities versus pressure. Columns 5 and 6 of Table II show that the relationship of  $I_{\nu_{\max}}$  to  $\Sigma I$  is quite linear over the range of relative humidities investigated. However, the relation of the entries in these columns to the gravimetric quantities in column 2 (Table II) deviates significantly from linearity above 1.3% relative humidity.

The heats of adsorption and desorption estimated from the isotherms are illustrated in Figs 7 and 8, respectively. The heats appear to be significantly temperature-dependent. In addition, the heats appear to be significantly dependent on coverage below 0.15 g of water per g of gel. The shape of the adsorption-heat curve (Fig. 7) is remarkably similar to that obtained for water adsorption on *O*-(carboxymethyl)cellulose, starch, and agar<sup>10</sup>.

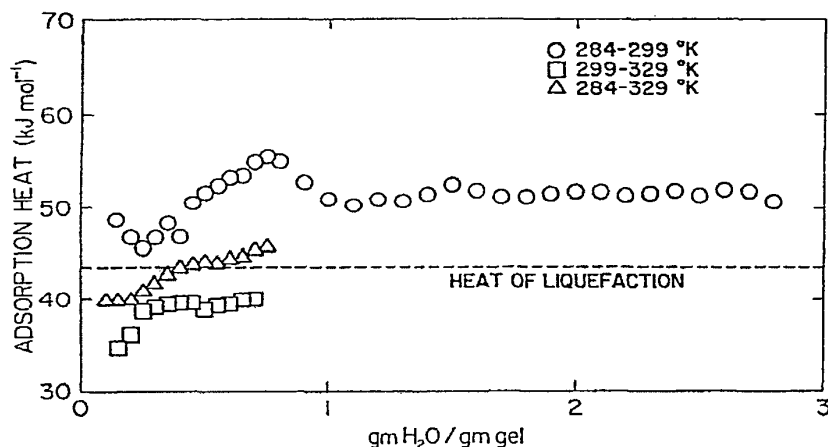


Fig. 7 Adsorption heats (exothermic) of water on dextran gel as a function of water coverage

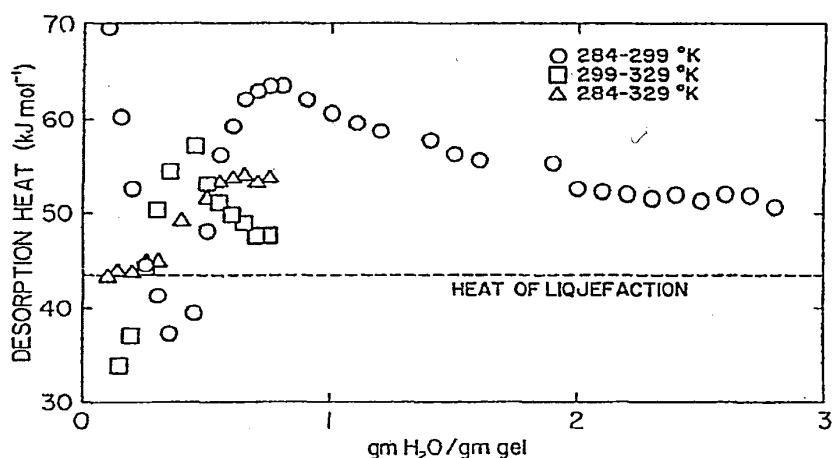


Fig. 8 Desorption heats (endothermic) of water on dextran gel as a function of water coverage.

*State of adsorbed water* — On the basis of the experimental evidence, the hydration process cannot be interpreted in terms of specific binding-sites. However,

as the following discussion indicates, the hydration mechanism is cooperative and involves both water-gel skeleton and water-water interactions. From a phenomenological point of view, sorption below 40% relative humidity ( $< 0.12$  g of water per g of gel) is characterized by several features: (a) The initial rotational relaxation (compare Fig. 4) is slower than inertial, but depends on the coverage. This *initial* relaxation, as characterized by  $t_{9\pi/200}$  (Table III, column 3), correlates directly with the total correlation time  $\tau_c$  (Table II, column 7) over the relative-humidity interval investigated, (b) the characteristic time for  $\pi/2$  diffusion ( $t_{\pi/2}$ , Table III, column 2) remains relatively constant ( $P/P_0 < 0.4$ ) at  $0.28 \pm 0.03$  picoseconds, and (c) the frequency of the  $\nu + \delta$  band-maximum (Table II, column 3) remains constant at about  $5184 \text{ cm}^{-1}$ . At the onset of saturation (above 40% relative humidity) the  $\pi/2$  diffusion slows considerably whereas the initial relaxation occurs more rapidly.

TABLE III

TIMES ( $t_{\pi/2}$ ,  $t_{9\pi/200}$ ) REQUIRED FOR INITIAL ROTATIONAL DIFFUSION THROUGH  $\pi/2$  AND  $9\pi/200$  RADIANS<sup>a</sup>

$P/P_0^b$	$t_{\pi/2} \times 10^{13} \text{ (sec)}^c$	$t_{9\pi/200} \times 10^{15} \text{ (sec)}^d$
0.007	3.10	10.00
0.013	2.79	7.82
0.028	2.85	8.71
0.061	2.75	7.99
0.086	2.68	7.74
0.129	2.71	7.74
0.169	2.71	8.16
0.271	2.71	7.31
0.363	2.94	7.23
0.436	2.41	7.05
0.550	4.28	7.23
0.679	4.94	6.65

<sup>a</sup>The term  $C(t)$  may be thought of as  $\cos \theta(t)$ , where  $\theta(t)$  is the angle between the transition-moment dipole at time  $t$  with respect to its orientation at time zero. The average angular-displacement as a function of time may be obtained from Fig. 3 by the relation  $\theta(t) = \cos^{-1} C(t)$ . <sup>b</sup> $P_0 = 22.4$  torr. <sup>c</sup>These were taken from Fig. 3, where  $C(t) = 10^{-3}$  or  $\theta = 89.95^\circ$ . <sup>d</sup>From Fig. 4,  $\theta = 8.1^\circ$ .

The constancy of the band maximum at  $5184 \text{ cm}^{-1}$  is particularly interesting, as the heat of adsorption is observed to vary by  $10 \text{ kJ mol}^{-1}$ . In addition, it may be noted that a significant, spherically symmetric, vibrational perturbation is operating in that  $5184 \text{ cm}^{-1}$  is  $107 \text{ cm}^{-1}$  lower than the band-center position of critical water<sup>33</sup> (which is a vibrationally unperturbed situation). The question thus arises as to the nature of the binding between the water and the gel. Hydrogen bonds formed by the water acting as a donor are expected to perturb the  $\nu + \delta$  vibrational band-center strongly, whereas the perturbing effects of hydrogen bonds formed with the water acting as an acceptor are expected to be small (compare  $\nu_2$  and  $\nu_3$  normal modes). As the observed band-center does not shift markedly with varying coverage

or heat of adsorption, but is shifted initially by  $-107 \text{ cm}^{-1}$ , singular donor or acceptor attachments can probably be ruled out. The  $-107 \text{ cm}^{-1}$  vibrational shift is attributed simply to the "skeletal field" of the gel and it is proposed that the adsorbed water molecules participate in two (or more) "hydrogen bonds" (involving gel hydroxyl groups and/or ether linkages). The vibrational restriction is, on the average, fairly constant and quite close (at all coverages) to that observed<sup>32</sup> in bulk water ( $\bar{\nu}_{\text{max}}$  for bulk water is  $5181 \text{ cm}^{-1}$ ). The variation of heats of adsorption with coverage must therefore be ascribed to differences in (the magnitudes of) the *spherically symmetric* components of the skeletal (potential) field. The variations observed in the heats in the interval 0.02–0.15 g of water per g of gel indicates that the adsorption may be cooperative in nature. This cooperativity might be induced by minor skeletal distensions and by additional dipolar contributions to the skeletal field induced by the adsorbed water molecules.

The correlation times  $\tau_c$  correlate directly with the  $t_{9\pi/200}$  value. This is not surprising, as the initial decay ( $<0.2 \text{ psec}$ ) makes the most significant contribution to the integrated relaxation-time. The effective inertance at time zero of the bound water reflects (in part) the *strength* of the adsorption.

In addition to the qualitative features (initial decay, inflection at 0.1–0.2 psec,  $\pi/2$  diffusion) of the correlation functions already discussed, the *oscillatory* components of the  $C(t)$  may be analyzed to obtain information about the angular perturbations. The frequencies,  $\langle \Delta\omega \rangle$ , of the beats observed in the  $C(t)$  have been shown<sup>33</sup> to be related to the vibrational band-center shifts ( $\Delta\omega_v$ ) and average angular perturbations ( $\langle \Delta\omega_{\phi} \rangle$ ) by the relation

$$\langle \Delta\omega \rangle = \langle \Delta\omega_{\phi} \rangle - \Delta\omega_v.$$

The average perturbation-frequencies  $\langle \Delta\omega_{\phi} \rangle$  are averages of the differences between the perturbed rotational-energies in the ground and excited vibrational levels. As is apparent from Figs. 3-a, -b, and -c, the beat frequencies  $\langle \Delta\omega \rangle$  are also time-dependent. This time-dependence relates directly to the time-dependence of  $\langle \Delta\omega_{\phi} \rangle$  and indicates that the non-spherically symmetric, angular potential-field perturbs the motion of the water differently depending on the relative orientations. The angular-perturbation frequencies for the first two beats are listed in Table IV as a function of coverage, and are compared with values characteristic of bulk water and water adsorbed on zeolite (an aluminosilicate) and silica. The frequencies are negative, because the non-spherically symmetric, rotational levels in the excited vibrational state are stabilized by the perturbing potential-field more than the corresponding rotational levels in the ground vibrational state<sup>33</sup>. This is evidenced by the tailing to lower frequencies of the  $(\nu + \delta)$  bands (Fig. 2). As illustrated in Table IV, increasing coverage results in increasing angular perturbation during the first "beat" (which correlates roughly with the decreasing initial inertance). The second "beats" indicate smaller perturbation with increasing coverage. The average of (first and second beats) the listed  $\langle \Delta\omega_{\phi} \rangle$  remains fairly constant ( $280 \pm 12 \text{ cm}^{-1}$ ) and differs by 200–400  $\text{cm}^{-1}$  from the other water examples listed in the table. On this basis, we would predict that the 650–



TABLE IV

AVERAGE ANGULAR-PERTURBATION FREQUENCIES,  $\langle \Delta\omega_{\delta\phi} \rangle$ ,  
AND CHARACTERISTIC  $\pi/2$  ROTATIONAL FREQUENCIES,  $\omega_{\pi/2}$ ,  
AS A FUNCTION OF COVERAGE ( $P/P_0$ ) FOR  $H_2O$  ( $\nu + \delta$ ) BAND

$P/P_0^a$	$\langle \Delta\omega_{\delta\phi} \rangle^a (cm^{-1})$		$\omega_{\pi/2}^d (cm^{-1})$
	(1) <sup>b</sup>	(2) <sup>c</sup>	
0.007	-246	-325	108
0.013	-256	-289	120
0.028	-252	-301	117
0.061	-262	-297	121
0.086	-269	-269	124
0.129	-269	-287	123
0.169	-278	-270	123
0.271	-300	-283	123
0.363	-305	-259	113
0.436	-312	-252	139
0.550	-286	-282	78
0.697	-315	-253	68
Bulk water (30°C) <sup>e</sup>	-584	-732	<200
Water sorbed in zeolite <sup>e, h</sup>	-406	-491	<100
Water adsorbed on silica <sup>e, i</sup>	-460	-484	~100
OH Raman stretch (bulk) <sup>f</sup>	—	—	176

<sup>a</sup> $P_0 = 22.4$  torr <sup>b</sup>Calculated from period of first "beat" <sup>c</sup>Calculated from period of second "beat"  
<sup>d</sup>Calculated from  $\pi/2$  values (see Table III) <sup>e</sup>Ref 33 <sup>f</sup>Ref 36 <sup>g</sup>Vibrational shifts ( $\Delta\omega$ ) relative to  
critical water (5291  $cm^{-1}$ ) <sup>h</sup>1 ml  $H_2O/g$  zeolite (Type A) at 25°C <sup>i</sup>Water-saturated silica (HiSil) at  
25°C, silica heat-treated at 800°C (see Ref 42)

750  $cm^{-1}$  "librational" band of bulk water should appear in the 280–300  $cm^{-1}$  region for water adsorbed on the gel

Consideration of the characteristic  $\pi/2$  diffusion times (Table III) and their associated frequencies (Table IV) yields additional information on the microdynamical behavior of the adsorbed water. It was noted earlier that  $t_{\pi/2}$  undergoes a jump at coverages corresponding to the onset of saturation. Bulk water has a characteristic "librational" mode at about 175  $cm^{-1}$ , which corresponds to  $\pi/2$  diffusion [compare, bulk ( $\nu + \delta$ ) and Raman OH  $\omega_{\pi/2}$  in Table IV]. This mode is predicted to be displaced to about 120  $cm^{-1}$  in the gel.

Although information related to enthalpies is obtained from analysis of the correlation functions, the information contained in these functions is more fundamentally entropic with regard to the state of the water in the adsorbed phase. This is especially true as regards the rotational entropy (freedom), although the small rotational barrier and the  $\omega_{\pi/2}$  imply indirectly a certain amount of translational freedom also.

In a study by Masuzawa and Sterling<sup>10</sup> of water sorption in several carbo-

hydrate gels, it was shown that the shapes of the (adsorption) entropy *vs.* coverage curves were almost identical to those of the heats of adsorption. The shapes of the isotherms obtained here (Fig. 6), when plotted against  $P/P_0$  linearly rather than logarithmically, are similar to those obtained by the authors mentioned. On this basis it is expected that the (water) adsorption entropy of the dextran gel should show the same general curvature as the adsorption heats. This was confirmed as illustrated in Table V for the representative coverages of 0.026, 0.075, and 0.110 g of water per g of gel. The first and third coverages (compare Fig. 7) correspond to major relative minima in the adsorption-heat curve and the second corresponds to a relative maximum. The differential entropy ( $\Delta\bar{S}$ ) is the adsorption entropy, and the isosteric adsorption-heat (Fig. 7) is equivalent to the differential enthalpy. The parallel course of the entropy and enthalpy reiterates the cooperative nature of the water adsorption. It is interesting to speculate as to which of the degrees of freedom contributes to the adsorption entropy. The vapor-phase rotational and translational entropies are given in Table V. From the experimental adsorption-entropy  $\Delta\bar{S}_{\text{exp}}$  (Table V), it may be concluded that a substantial part of translational entropy has been lost. The restric-

TABLE V

EXPERIMENTAL<sup>a</sup> MOLAR AND DIFFERENTIAL ADSORPTION-ENTROPIES AND GAS-PHASE ROTATIONAL AND TRANSLATIONAL ENTROPIES AT REPRESENTATIVE COVERAGES

Coverage (g H <sub>2</sub> O/g gel)	$-\Delta\bar{S}_{\text{exp}}^b$ (J°K <sup>-1</sup> mol <sup>-1</sup> )	$-\Delta\bar{S}_{\text{exp}}^c$ (J°K <sup>-1</sup> mol <sup>-1</sup> )	$S_{\text{calc}}^{\text{rot } d e}$ (J°K <sup>-1</sup> mol <sup>-1</sup> )	$S_{\text{calc}}^{\text{trans } f}$ (J°K <sup>-1</sup> mol <sup>-1</sup> )
0.020	148			
0.026	146	150	46.3	200.3
0.030	150			
0.071	175			
0.075	177	182	46.3	190.3
0.079	176			
0.106	160			
0.110	158	153	46.3	186.2
0.114	159			

<sup>a</sup>From the runs at 284 and 299°K, temperature of 291.5°K used throughout in calculations. <sup>b</sup>Molar adsorption-entropy (see Refs. 43 and 44) calculated from isosteric heats (Fig. 7) and adsorption isotherms (Fig. 6) according to the equation  $\Delta\bar{S} = -\frac{R}{n} \int_0^n d\ln(P/P_0) + \Delta H^{\text{ads}}/T$ , where  $R$ ,  $T$ , and  $n$  respectively are the gas constant, temperature, and coverage. <sup>c</sup>Differential adsorption-entropy (Ref. 43) calculated from  $\Delta\bar{S}$  according to the equation  $\Delta\bar{S} = n \frac{d\Delta\bar{S}}{dn} + \Delta\bar{S}$ . <sup>d</sup>Calculated by using (Refs. 45 and 46) the partition function  $q^{\text{rot}} = \frac{\sqrt{\pi}}{2} \left( \frac{8\pi^2 I_A kT}{h^2} \right)^{1/2} \left( \frac{8\pi^2 I_B kT}{h^2} \right)^{1/2} \left( \frac{8\pi^2 I_C kT}{h^2} \right)^{1/2}$ , which yields the expression (after evaluating all constants)  $S^{\text{rot}} = 12.47 \ln T - 24.44$  (J°K<sup>-1</sup> mol<sup>-1</sup>). <sup>e</sup>Equipartition of  $S^{\text{rot}}$  according to the three principal moments gives  $S_{I_A}^{\text{rot}}$ ,  $S_{I_B}^{\text{rot}}$ , and  $S_{I_C}^{\text{rot}}$  respectively as 13.11, 15.72, and 17.50 (J°K<sup>-1</sup> mol<sup>-1</sup>). <sup>f</sup>Calculated by using (Refs. 45 and 46) the partition function  $q^{\text{trans}} = \left( \frac{2\pi[2m_B + m_0]}{h^2} \right)^{3/2} V$ , which gives  $S^{\text{trans}} = 20.79 \ln T - 8.31 \ln p + 26.36$  (J°K<sup>-1</sup> mol<sup>-1</sup>), where  $p$  is expressed in atmospheres.

tions of the rotational motion observed through the higher-than-inertial relaxation should also lead to some loss of rotational entropy. The proportion of these two losses is uncertain, but it is likely that the variations of the adsorption entropy with surface coverage are caused by rotational contributions only

At coverages greater than about 0.12 g of water per g of gel, the gel begins to become saturated (compare Fig 6), and the condensed water begins to impede its own motion (compare Fig 3-c). That saturation sets in at this low coverage (0.12 g of water per g of gel corresponds roughly to one water molecule per glucose monomer) indicates that the hydroxyl groups of glucose must be heavily involved in intermolecular or intramolecular hydrogen-bonding. This is supported by the i.r. evidence (compare Table I), as the OH band-maximum at  $3400\text{ cm}^{-1}$  is characteristic of hydrogen-bonded hydroxyl groups whereas the free hydroxyl-group stretch is usually found  $200\text{ cm}^{-1}$  higher. This same equivalence (1 water molecule per glucose residue) at the onset of saturation is in agreement with a previous study of dextran hydration<sup>18</sup> and a hydration study of several other carbohydrate polymers<sup>10</sup>

#### ACKNOWLEDGMENTS

The authors are indebted to Professors W. E. Ohnesorge and J. R. Merkel for their gift of the dextran gel. Thanks are also due the L. U. Computing Center for a generous grant of computing time. The authors would also like to express their sincere thanks to two of the referees for several criticisms and suggestions regarding this paper.

#### REFERENCES

- 1 P. H. HERMANS, *Contribution to the Physics of Cellulose Fibers*, Elsevier, Amsterdam, 1946
- 2 H. J. WHITE AND H. EYRING, *Textile Res. J.*, 17 (1947) 523
- 3 A. D. McLAREN AND J. W. ROWEN, *J. Polymer Sci.*, 7 (1951) 289
- 4 T. M. SHAW AND R. H. ELSKEN, *J. Chem. Phys.*, 21 (1953) 565
- 5 T. M. SHAW AND R. H. ELSKEN, *Anal. Chem.*, 27 (1955) 1983
- 6 R. COLLISON AND M. P. McDONALD, *Nature*, 186 (1960) 548
- 7 M. J. TAIT, S. ABLETT, AND F. W. WOOD, *J. Colloid Interface Sci.*, 41 (1972) 594
- 8 K. KAINUMA AND D. FRENCH, *Biopolymers*, 11 (1972) 2241
- 9 M. K. S. MORSE, C. STERLING AND D. H. VOLMAN, *J. Appl. Polym. Sci.*, 11 (1967) 1217.
- 10 M. MASUZAWA AND C. STERLING, *J. Appl. Poly. Sci.*, 12 (1968) 2023
- 11 S. L. GUPTA AND R. K. S. BHATIA, *Indian J. Chem.*, 7 (1969) 1231
- 12 B. DAS, R. K. SETHI, AND S. L. CHOPRA, *Israel J. Chem.*, 10 (1972) 963
- 13 N. W. TAYLOR, J. E. CLUSKEY, AND F. R. SENTI, *J. Phys. Chem.*, 65 (1961) 1810
- 14 N. W. TAYLOR, H. F. ZOBEL, M. WHITE, AND F. R. SENTI, *J. Phys. Chem.*, 65 (1961) 1816
- 15 D. H. NORTHCOTE, *Biochim. Biophys. Acta*, 11 (1953) 471.
- 16 O. HECHTER, T. WITTSTUCK, N. MCNIVEN, AND G. LESTER, *Proc. Natl. Acad. Sci. U. S.*, 46 (1960) 783
- 17 P. C. NICOLSON, G. U. YUEN, AND B. ZASLOW, *Biopolymers*, 4 (1966) 677
- 18 N. W. TAYLOR, H. F. ZOBEL, N. N. HELLMAN, AND F. R. SENTI, *J. Phys. Chem.*, 63 (1959) 599.
- 19 *Literature References*, 1959-1972 (Nos 1-4076), 1973 (Nos 4077-4671), 1974 (Nos 4672-5265), Pharmacia Fine Chemicals Inc., Rahms Lund, Sweden
- 20 N. V. B. MARSDEN, *Ann. N. Y. Acad. Sci.*, 125 (1965) 428
- 21 D. ABBOT, E. J. BOURNE, AND H. WEIGEL, *J. Chem. Soc.*, (1966) C827

- 22 O LARM, B LINDBERG, AND S SVENSSON, *Carbohydr Res*, 20 (1971) 39
- 23 E J BOURNE, R L SIDFBOTHAM, AND H WEIGEL, *Carbohydr Res*, 22 (1972) 13.
- 24 H MIYAJI AND A. MISAKI, *Carbohydr Res*, 31 (1973) 277
- 25 W B NEELY, *Advan Carbohydr Chem*, 15 (1960) 341
- 26 W B NEELY, *Advan Carbohydr Chem*, 12 (1957) 13
- 27 P D VASKO, J BLACKWELL, AND J L KOENIG, *Carbohydr Res*, 19 (1971) 297
- 28 P. D VASKO, J. BLACKWELL, AND J. L KOENIG, *Carbohydr Res*, 23 (1972) 407
- 29 E NEMES-NANASI, *Acta Biol. Debrecina*, 5 (1967) 67
- 30 E NEMES-NANASI, *Acta Biol. Debrecina*, 6 (1968) 89
- 31 G A KOGAN, V M TUL'CHINSKY, M. L SHULMAN, S E ZURABYAN, AND A. YA KHEORLIN, *Carbohydr Res*, 26 (1973) 191.
- 32 K. KLIER, J H SHEN, AND A C ZETTLEMOYER, *J Phys Chem*, 77 (1973) 1458.
- 33 K. KLIER, *J Chem Phys*, 58 (1973) 737
- 34 R G GORDON, *J Chem Phys*, 43 (1965) 1307
- 35 J A TEXTER, K. Klier, AND A C ZETTLEMOYER, *Prog Surface and Membrane Sci*, in press
- 36 T. T WALL, *J Chem Phys*, 51 (1969) 113
- 37 J W MCBAIN AND A M BAKR, *J Amer Chem Soc*, 48 (1926) 690
- 38 K KLIER, *Catal Rev*, 1 (1967) 207
- 39 K. KLIER, *J. Opt Soc Amer*, 62 (1972) 882.
- 40 G KORTUM, *Reflectance Spectroscopy*, Springer-Verlag, New York, 1969
- 41 G HERZBERG, *Molecular Spectra and Molecular Structure II Infrared and Raman Spectra of Polyatomic Molecules*, Van Nostrand Reinhold Company, Toronto, 1945, p 448, Table 136, column 4
- 42 D R BASSETT, E A BOUCHER, AND A C ZETTLEMOYER, *J Colloid Interface Sci*, 28 (1968) 4
- 43 E K RIDEAL, *Surface Chemistry*, Cambridge Univ Press, 1930
- 44 R DEFAY, I PRIGOGINE, A BELLEMANS, AND D H EVERETT, *Surface Tension and Adsorption*, Wiley, New York, 1966
- 45 T. L HILL, *An Introduction to Statistical Thermodynamics*, Addison-Wesley, Reading, Mass, 1960
- 46 J D FAST, *Entropy*, McGraw-Hill, New York, 1962